Applied Catalysis B: Environmental 210 (2017) 444–453

Contents lists available at ScienceDirect

Applied Catalysis B: Environmental

journal homepage: www.elsevier.com/locate/apcatb

Revisiting the mechanism of hexavalent chromium ion reduction: The parallel photodecomposition and photocatalytic reduction of chromate(VI) ester

Fei Xu [a], Richard D. Webster [b], Jinfan Chen [a], Timothy T.Y. Tan [c], Patrick H.-L. Sit [a], Wey Yang Teoh [a,*]

[a] Joint Laboratory for Energy and Environmental Catalysis, Clean Energy and Nanotechnology (CLEAN) Laboratory, School of Energy and Environment, City University of Hong Kong, Kowloon, Hong Kong Special Administrative Region
[b] Division of Chemistry and Biological Chemistry, School of Physical and Mathematical Sciences, Nanyang Technological University, Nanyang Link, Singapore
[c] School of Chemical and Biomedical Engineering, Nanyang Technological University, Nanyang Drive, Singapore

ARTICLE INFO

Article history:
Received 2 December 2016
Received in revised form 24 March 2017
Accepted 6 April 2017
Available online 7 April 2017

Keywords:
Photocatalysis
Hexavalent chromium
Interfacial charge transfer
Density functional theory
Electron paramagnetic resonance

ABSTRACT

The formation and homogeneous photodecomposition of chromate(VI) ester are often overlooked during the studies of photocatalytic reduction of hexavalent chromium, Cr(VI), in the presence of sacrificial electron donors such as methanol. When photoexcited ($\lambda \leq 525$ nm), the chromate(VI) ester, formed by the spontaneous reaction of aqueous Cr(VI) with methanol, undergoes homogeneous stepwise decomposition to trivalent chromium, Cr(III). The addition of semiconductor photocatalysts, *i.e.*, TiO_2 and WO_3, at relatively low concentrations (<0.5 g L^{-1}) was detrimental to the overall rate of Cr(VI) reduction. This was traced to the occurrence of interfacial electron injection from chromate ester to the photocatalyst conduction band, that in turn interrupted inner sphere electron transfer, i.e., photodecomposition. Since it is an interfacial process, the extent of suppression of Cr(VI) reduction is more significant for highly adsorbing TiO_2 than on weakly adsorbing WO_3. At the same time, even though chromate ester adsorbs strongly on Al_2O_3, the interfacial electron injection to the insulator particle was unfavorable, and hence no suppression in Cr(VI) reduction was observed. When the TiO_2 photocatalyst concentration was increased to 0.5 g L^{-1} and beyond, the photocatalytic reduction path became dominant. Further increase in the photocatalyst concentration saw the linear dependency in the apparent rate of Cr(VI) reduction, as expected for reaction in the non-mass diffusion and non-light scattering limited region. As followed by the electron paramagnetic spectroscopy, both the photodecomposition and photocatalytic reactions follow the stepwise reduction from Cr(VI) to Cr(V) and eventually to Cr(III). For non-photoexcited TiO_2 ($\lambda \geq 420$ nm), suppression in the rate of Cr(VI) reduction was observed at all concentrations tested. Importantly, the work showcases the parallel but non-independent effects of homogeneous photodecomposition of chromate(VI) ester and its photocatalytic reduction over semiconductor photocatalysts.

© 2017 Elsevier B.V. All rights reserved.

1. Introduction

Leachate of toxic metals from landfills and industrial effluents is a serious environmental concern, where much of these metal ions end up in surface water sources in trace but potent concentrations [1]. Unlike other toxic metal ions such as Pb(II) and Hg(II) that have been banned altogether from many applications, hexavalent chromium (Cr(VI)) still finds widespread applications despite its carcinogenic and mutagenic nature [2,3]. It is an essential ingredient in many industrial applications including electroplating, leather tanning, and anti-corrosion steel. Because Cr(VI) is resistant to biodegradation, it tends to accumulate in living organisms, where its chronic exposure increases the risk of respiratory cancers in humans, [4–6] for instance, the formation of Cr(VI)-associated neoplasms in the lung, and nasal cancers [2,3,7,8]. As such the concentration of Cr(IV) in drinking water has been regulated at less than 50 ppb in many countries including Germany, Sweden, Argentina, and China [9,10].

The development of sustainable technologies for removing Cr(VI) from industrial effluents and securing safe drinking water is an ongoing challenge. In particular, photocatalysis is recognized as an effective and economical method of water decontamination.

* Corresponding author.
E-mail address: wyteoh@cityu.edu.hk (W.Y. Teoh).

http://dx.doi.org/10.1016/j.apcatb.2017.04.024
0926-3373/© 2017 Elsevier B.V. All rights reserved.

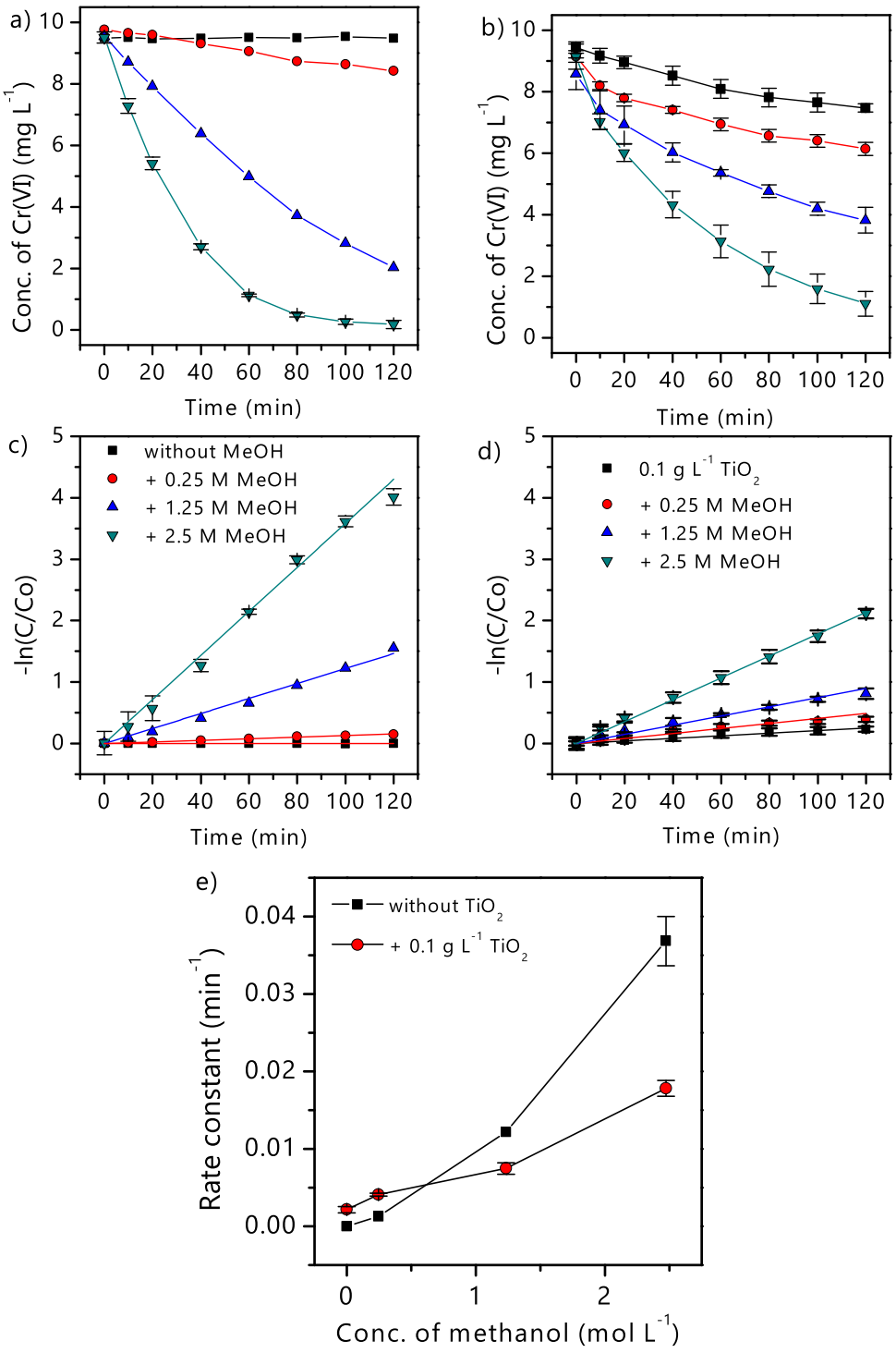

Fig. 1. (a) Homogeneous photoreduction (absence of solid catalysts) and (b) photocatalytic reduction (0.1 g L^{-1} TiO_2) of Cr(VI) as a function of methanol concentrations, as well as (c) and (d) the corresponding pseudo-first order rate plots. (e) The estimated rate constants with and without TiO_2 photocatalysts as a function of methanol concentrations. Initial Cr(VI) loading = 10 ppm, pH 3.0, N_2 saturated, Xe(Hg) full arc irradiation.

It is one of the core technologies for achieving a sustainable future based on solar energy [11–13]. When a photocatalyst is irradiated with photons of energy equal to or larger than the bandgap energy, electron-hole pairs are generated and followed by diffusion to the surface to catalyze redox reactions. Because of the parallel charge trapping and recombination processes, the amount of net usable photocharges depends on the relative kinetics of each of the charge transport processes [14]. During the photocatalytic oxidation of organic pollutants, molecular oxygen is introduced as an efficient photoelectron scavenger. However, in the event of photocatalytic reduction, such as the reduction of Cr(IV) to Cr(III) in this particular study (Eq. (3.1)), the oxidation of water to molecular oxygen is the electron donating reaction unless sacrificial electron donors are introduced to scavenge the photoholes:

$$Cr_2O_7^{2-} + 14H^+ + 6e^- \Leftrightarrow 2Cr^{3+} + 7H_2O E^\circ = +1.33\,V vs.RHE \quad (3.1)$$

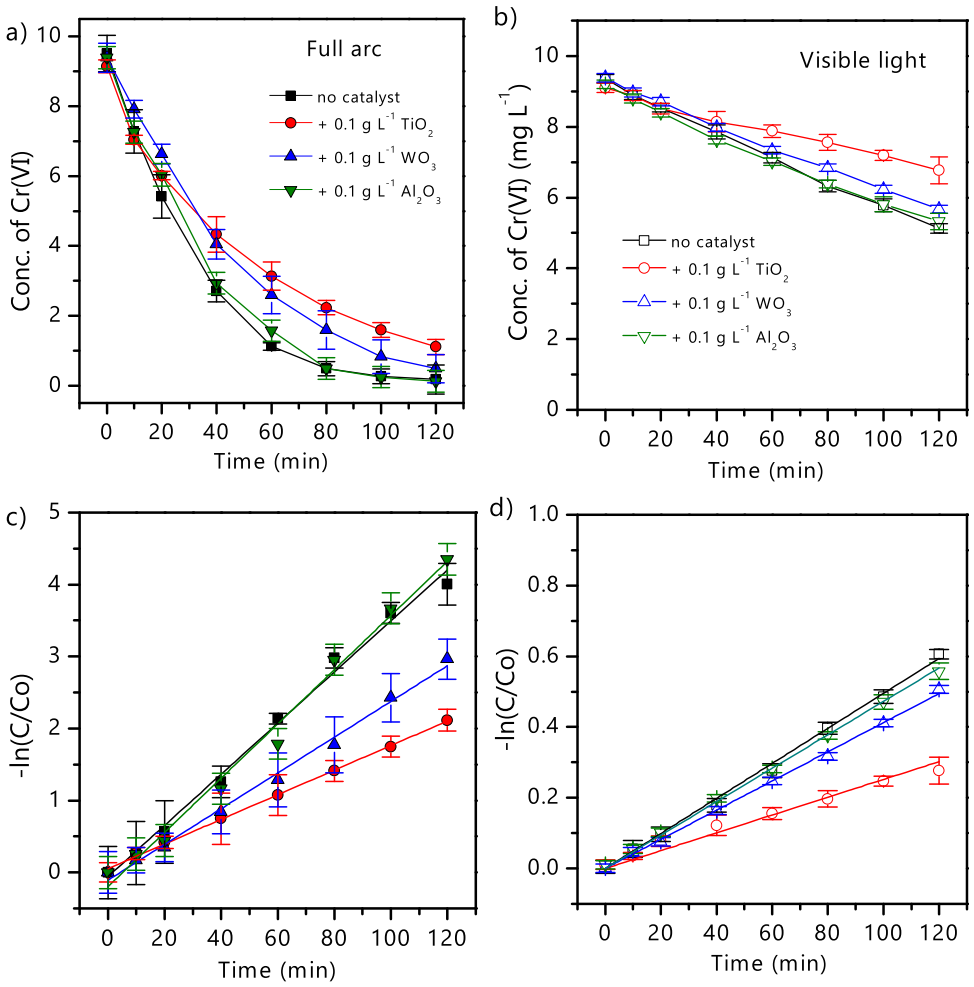

Fig. 2. Photocatalytic reduction of Cr(VI) over 0.1 g L^{-1} TiO_2, WO_3 and Al_2O_3 under (a) full arc and (b) visible light ($\lambda \geq 420$ nm) irradiation, as well as (c) and (d) the corresponding pseudo-first order rate plots. Initial Cr(VI) loading = 10 ppm, pH 3.0, N_2 saturated, 2.5 M methanol.

Compared to other oxidation states of Cr ions, Cr(III) is a relatively benign product with significantly lower toxicity since it can be excreted from human body.

Organics such as alcohols, [15,16] organic acids, [16–18] humic acid, [19,20] phenols, [16,18] and EDTA [16,21] are frequently added as electron donors to substitute the sluggish four-electron oxidation of water, and hence accelerate the overall kinetics of reduction [11]. Despite alcohols being one of the most commonly employed sacrificial donor, a fundamental aspect that is often overlooked is the formation of photosensitive chromate(VI) ester that is subjected to photoreduction even in the absence of photocatalysts [22–25]. The occurrence of such homogeneous reaction in parallel to the heterogeneous photocatalytic electron transfer complicates the overall mechanism of Cr(VI) reduction, and to some extent confuses the kinetic measurements. The occurrence of both mechanisms ought to be elucidated in the interest of identifying the most efficient remediation path.

Herein, we investigate the formation of chromate(VI) ester from the reaction of Cr(VI) and methanol, and its simultaneous homogeneous and heterogeneous photoreduction. The role of the photocatalysts (*i.e.*, TiO_2 and WO_3) and the resultant photoinduced charge injection will be clarified, where under certain conditions, we identified the counter-productive presence of photocatalysts. This is mainly due to the undesirable interfacial charge injection that breaks the inner sphere ligand-to-metal charge transfer of the photodegradation of chromate(VI) ester. However when overcome, the photocatalytic reduction can potentially offer a more efficient remediation process.

2. Experimental

Photocatalytic reaction was carried out in the presence of Evonik P25 TiO_2 (48 m^2 g^{-1}) [26], WO_3 (14 m^2 g^{-1}) [27], or Al_2O_3 (82 m^2 g^{-1}, Buehler 0.05 μm), dissolved Cr(VI) ($NaCr_2O_7{\cdot}7H_2O$, >99.9%, Aldrich) and methanol (≥99.8%, Aldrich) in a pyrex reactor with circulated cooling water jacket (20 °C). For the homogeneous photodecomposition reaction, no photocatalyst was added to the reaction. The aqueous suspension was adjusted to pH 3.0 with diluted $HClO_4$ solution (>99.9%, Aldrich) or NaOH (>99.8%, Aldrich). The magnetically-stirred (800 rpm) suspension was continuously purged with air for aerated experiments, or with nitrogen for anoxic experiments. After 30 min of dark adsorption, the reduction of Cr(VI) was initiated by exposing the suspension to 200 W Xe(Hg) arc lamp (Newport). A 420 nm filter (Oriel GG 420) was placed in front of the lamp to provide visible light irradiation. The actual intensities of the light in front of the reactor was measured to be 220 and 120 mW cm^{-2} under full arc and visible light irradiation, respectively. Samples were drawn from the reactor at regular time intervals, and filtered through a syringe filter (Millipore, 0.2 μm pores, PTFE).

The concentrations of Cr(VI) were measured spectrophotometrically using the diphenyl carbazide (DPC) method [21]. A 60 μL of DPC reagent (prepared by dissolving 10 mg DPC in 2 mL ace-

tone, followed by adding 10 μL concentrated H_2SO_4) was added to 3 mL diluted sample solution and mixed. All the samples were incubated for 30 min before transferring to a quartz cell for the absorbance measurements in Shimadzu UV 3600 spectrophotometer. Continuous wave X-band electron paramagnetic resonance (EPR) spectra were recorded with a Bruker Elexsys E500 spectrometer. The quartz flat cell used allowed external full arc irradiation from a Xenon lamp upon a volume of solution approximately 1 ml. All EPR measurements were carried out using solutions of 1 ppm Cr(VI), 12.5 M methanol and 0.1 g L^{-1} photocatalysts (if applicable). Electron paramagnetic resonance spectra were recorded as first derivative curves.

DFT calculations were carried out using the gradient-corrected Perdew-Burke-Ernzerhof (GGA-PBE) functional [28] within the plane wave ultrasoft pseudopotential scheme as implemented in the Quantum-ESPRESSO package [29]. The plane-wave energy cutoffs are 30 and 240 Ry for the wave functions and the augmented charge density, respectively. Reciprocal space was sampled at the Γ point. The TiO_2 (101) surface was modeled as a slab geometry in the anatase structure with the experimental lattice parameter to be a = b = 4.59 Å, c = 2.96 Å [30]. In the construction of the slab, we adopted a supercell with 36 Ti and 72 O ions. The slab is ~8.9 Å thick and the vacuum length was chosen to be 10 Å. The surface of WO_3 (002) was built with the experimental lattice parameter of the crystal with a = 7.69 Å, b = 7.54 Å, c = 10.52 Å, and β = 136.06 Å [31]. The slab model is ~16.7 Å thick with the vacuum length to be 20 Å. The supercell contains 64 W and 192 O ions. The adsorption model was constructed with the chromate(VI) ester binding on the TiO_2 (101) or the WO_3 (002) surface.

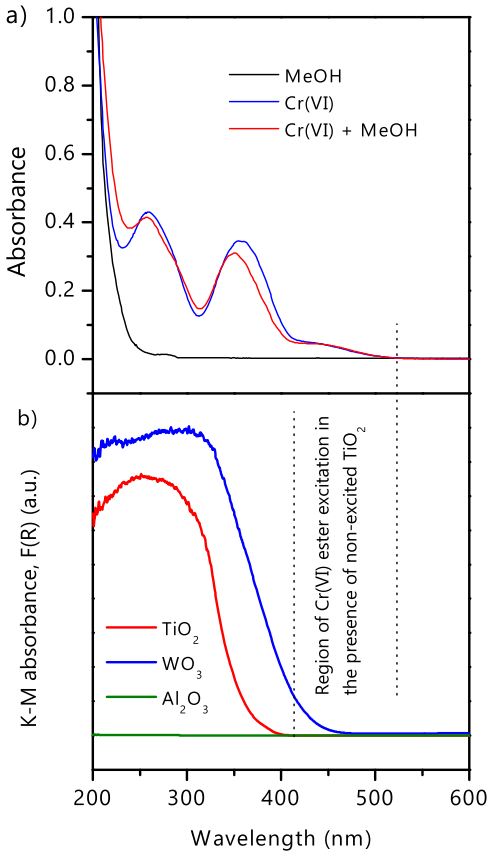

Fig. 3. (a) Optical absorbance of aqueous 10 ppm Cr(VI), 10 ppm Cr(VI) + 2.5 M methanol, and 2.5 M methanol adjusted to pH = 3.0; and (b) the Kubelka-Munk absorbance of TiO_2, WO_3 and Al_2O_3.

3. Results and discussion

As shown in Fig. 1a and c (black square), the aqueous solution of Cr(VI) on its own cannot be reduced under full arc irradiation. The addition of 0.1 g L^{-1} TiO_2 (Fig. 1b and d, black square) resulted in the photocatalytic reduction of Cr(VI) despite a relatively sluggish rate (pseudo-first order rate constant, $k = 0.002 \pm 0.0005$ min^{-1}) that is limited strongly by the kinetics of water oxidation [32–34]. As such, the addition of methanol accelerated the photocatalytic reduction of Cr(VI) following the simple first order reaction kinetics with respect to the methanol concentration. However, as noted in Fig. 1a and c, the homogeneous photodecomposition of Cr(VI) in the absence of photocatalyst also increases with increasing methanol concentration (Fig. 1e). A higher order of dependencies with respect to methanol concentration can actually be measured compared to that in the presence of TiO_2 photocatalyst indicating a different reaction mechanism (Fig. 1e). In fact, the Cr(VI) reduction was drastically hampered by the presence of TiO_2 at the methanol concentration of ~0.65 M and above. This is counter-intuitive to the additional effect of photocatalytic reduction of Cr(VI) as contributed by the TiO_2, even in the excess of methanol in all cases (*e.g.*, MeOH:Cr(VI) molar ratio = 1300, at 0.25 M methanol). By replacing the TiO_2 photocatalyst suspension with that of Al_2O_3 insulator, the standard control for non-photocatalytic material, we rule out the

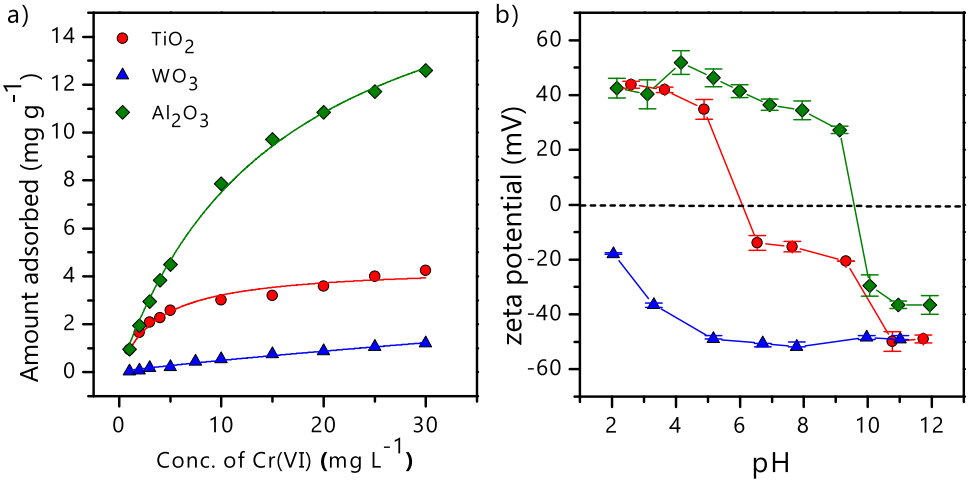

Fig. 4. (a) Langmuir adsorption isotherm of Cr(VI) on TiO_2, WO_3 and Al_2O_3 at pH 3.0; and (b) the zeta potential TiO_2, WO_3 and Al_2O_3 measured as a function of suspension pH.

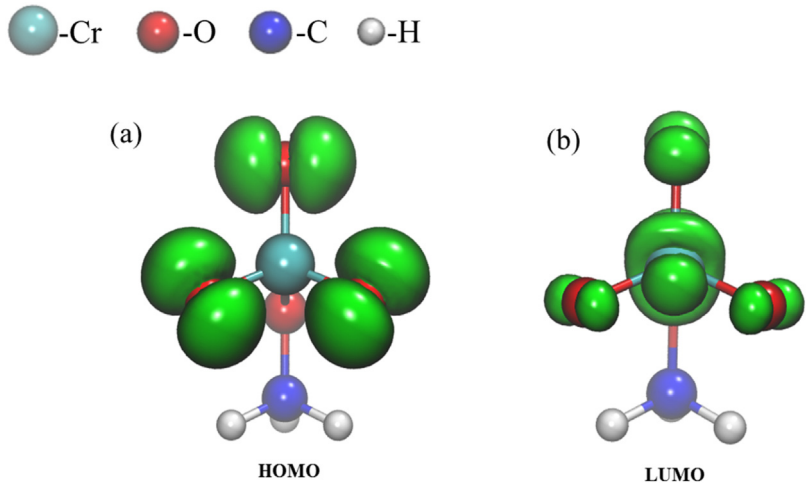

Fig. 5. The charge densities of the (a) HOMO, (b) LUMO states of the isolated chromate(VI) ester. The charges density contours are in green. The HOMO localizes on the three oxygen atoms covalently bonded to the chromium, and the LUMO has significant contribution from the chromium ion.

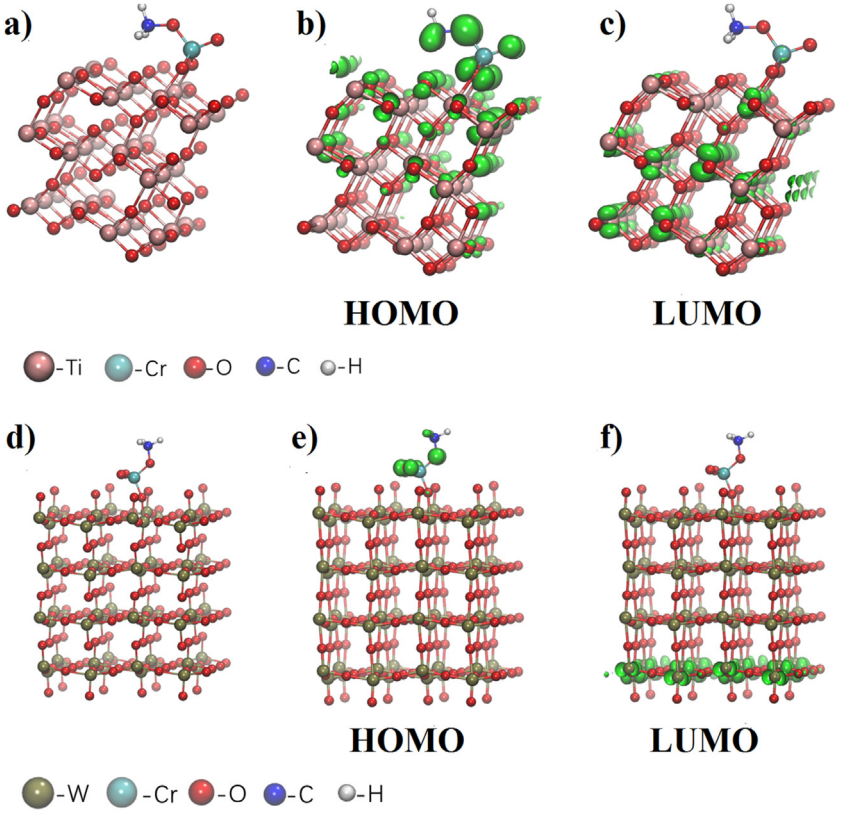

Fig. 6. (a) Optimized geometry of the chromate(VI) ester adsorbed on TiO_2 (101) surface, and the charge density (green) of the (b) HOMO and (c) LUMO states. (d) Optimized geometry of the chromate(VI) ester adsorbed on WO_3 (002) surface, and the charge density (green) of the (e) HOMO and (f) LUMO states. (For interpretation of the references to colour in this figure legend, the reader is referred to the web version of this article.)

effect of light scattering as the cause for the reduction in photoactivity (discussed below).

As shown in Fig. 2a and c, there is no obvious difference in the reduction rate of Cr(VI) from the homogeneous photodecomposition of chromate(VI) ester with or without Al_2O_3. Up to this end, the results suggest that the suppressed activity from the addition of TiO_2 must arise from another reaction pathway. As shown in Fig. 3, the chromate(VI) ester is capable of absorbance in the visible range up to 525 nm, where TiO_2 is incapable of photoexcitation. We verified that irradiation at $\lambda \geq 550$ nm did not result in the reduction of chromate(VI) ester (Fig. S1). This presents an irradiation window (*i.e.*, $420 \leq \lambda \leq 525$ nm) within which one can evaluate the effect chromate(VI) reduction in the presence of non-excited TiO_2, *i.e.*, no photocatalytically-generated charge carriers. Despite the subtle difference in the optical absorbance between the aqueous chromate(VI) (denoted Cr(VI) in Fig. 3) and that of chromate(VI) ester (denoted Cr(VI) + MeOH in Fig. 3), the latter matches with the experimental and theoretical spectrum reported by Kaufman and Weber [35]. The homogeneous reduction of Cr(IV) in the presence of methanol continues to be measured under visible light ($\lambda \geq 420$ nm) with a pseudo-first order rate constant, $k = 0.036 \pm 0.001$ min^{-1}, almost indifferent from that of the

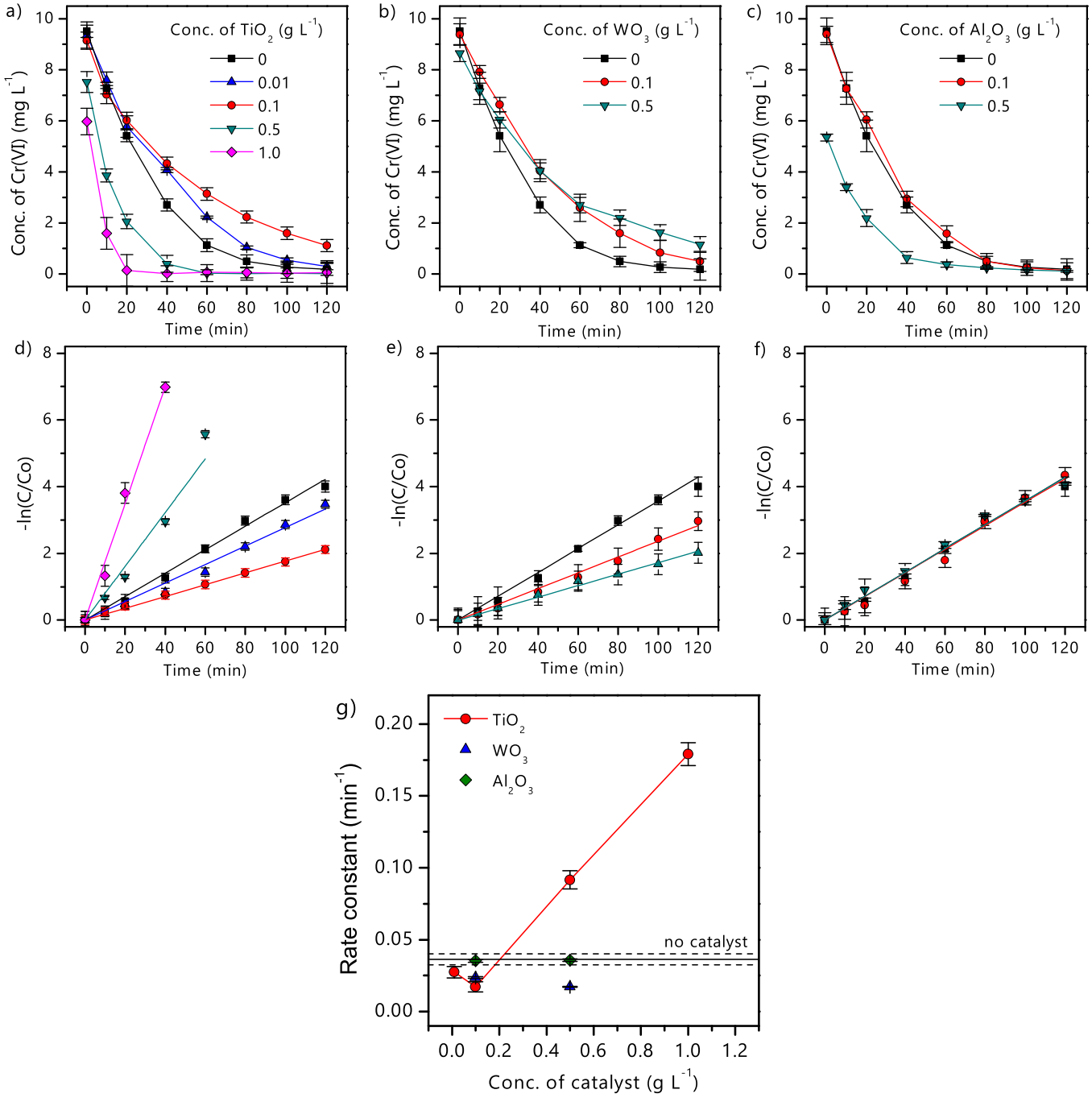

Fig. 7. The photocatalytic reduction of Cr(VI) at different loadings of (a) TiO_2, (b) WO_3, (c) Al_2O_3 under full arc irradiation, and (d)–(f) the corresponding pseudo first-order rate plots. (g) The estimated rate constants as a function of the different photocatalyst loadings. The solid horizontal line (standard deviation in broken horizontal lines) representing the rate constant in the absence of photocatalysts is included in (g) for comparison. Initial Cr(VI) loading = 10 ppm, pH 3.0, N_2 saturated, 2.5 M methanol, Xe(Hg) full arc irradiation.

Al_2O_3 control, $k = 0.035 \pm 0.001\ min^{-1}$ (Fig. 2b and d). Under the same condition, the suppression of Cr(VI) reduction was measured in the presence of non-photoexcited TiO_2 by up to 2-fold ($k = 0.018 \pm 0.0004\ min^{-1}$). A plausible mechanism is the interfacial electron injection from the photoexcited chromate(VI) ester to the conduction band of TiO_2. Under normal photodecomposition, that is, without the presence of TiO_2, the photoexcitation of chromate(VI) ester is known to undergo the inner sphere ligand-to-metal charge transfer (LMCT) [35–37], where the photoelectrons would reduce the Cr(VI) center [34]. Instead, the presence of TiO_2 draws the electrons from the chromate(VI) ester through the interfacial charge injection and hence preventing the net photoreduction of the Cr(VI) centre. Similarly, as shown in Fig. 2, the photoreduction of Cr(VI) reduction in the presence of WO_3 was suppressed under both full arc and visible light irradiation although to a smaller extent than TiO_2. In summary, we observe the same Cr(VI) reduction activity trend in the order of no catalyst = Al_2O_3 > WO_3 > TiO_2 regardless of the irradiation sources.

To substantiate the hypothesis above, one of the underlying requirements for the interfacial charge transfer is the adsorption of the chromate(VI) ester on the photocatalyst. Fig. 4a shows the Langmuir adsorption isotherm of Cr(VI) on the TiO_2, WO_3 and

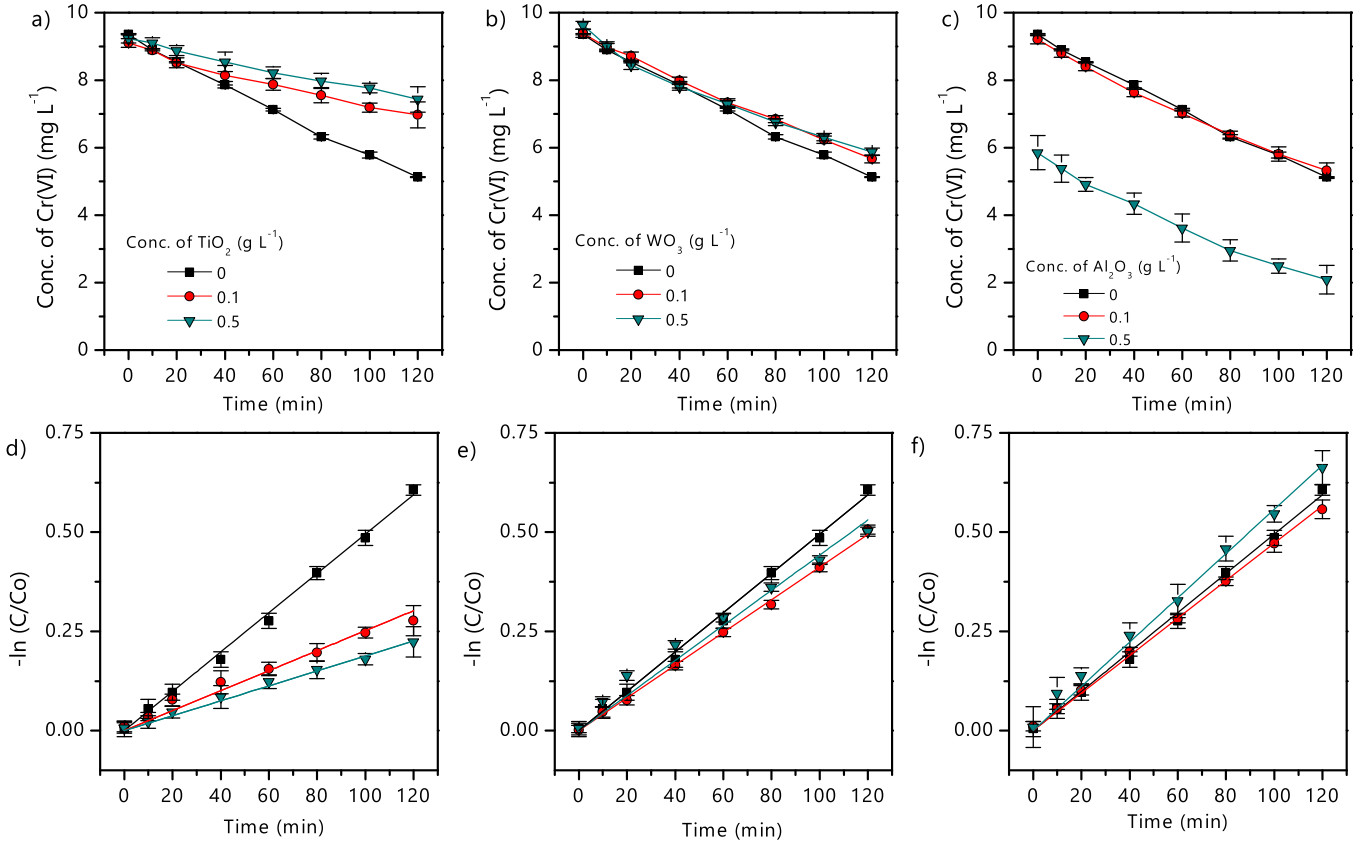

Fig. 8. The photocatalytic reduction of Cr(VI) at different loadings of (a) TiO_2, (b) WO_3, (c) Al_2O_3 under visible light ($\lambda \geq 420$ nm) irradiation, and (d)–(f) the corresponding pseudo first-order rate plots. Initial Cr(VI) loading = 10 ppm, pH 3.0, N_2 saturated, 2.5 M methanol, Xe(Hg) arc lamp with 420 nm cutoff filter.

Al_2O_3 suspensions. At pH 3.0, the Cr(VI) exists predominantly as chromate(VI) ions ($HCrO_4^-$) [22,38], which is analogous to the negatively charged chromate(VI) ester. Under this condition, the saturation adsorption of chromate(VI) on TiO_2, WO_3 and Al_2O_3 was estimated to be 4.4 mg g TiO_2^{-1}, 1.8 mg g WO_3^{-1} and 19.4 mg g $Al_2O_3^{-1}$, respectively. The adsorption capacity trend can be adequately explained by the surface charge of the metal oxide particles. From the zeta potential plot in Fig. 4b, the TiO_2 and Al_2O_3 surfaces are positively-charged at pH 3.0, allowing the chromate(VI) to be electrostatically adsorbed, while electrostatic repulsion minimized the adsorbed on the negatively-charged WO_3 surface. In other words, although the chromate(VI) adsorption on Al_2O_3 is favorable, its insulating nature prevented the interfacial charge injection from taking place, and hence no effect on the kinetics of photodecomposition of chromate(VI) ester could be measured compared to the pure homogeneous system (Fig. 2). On the contrary, the conduction band edge potentials of TiO_2 (−0.5 V *vs.* RHE, pH 0) [39] and WO_3 (+0.4 V *vs.* RHE, pH 0) [40,41] are favorable for the interfacial charge injection, but the latter is impaired by the weak surface adsorption of chromate(VI).

To provide microscopic insights into the photoreduction process of the chromate(VI) ester, we studied the electronic structures of the isolated chromate(VI) ester and of its adsorption models on the TiO_2 and WO_3. As shown in Fig. 5, the highest occupied molecular orbital (HOMO) of the isolated chromate(VI) ester mainly situates on the three oxygen atoms bonded to the chromium ion, while a significant contribution to the lowest unoccupied molecular orbital (LUMO) comes from the chromium ion. This corroborates the favorable intramolecular electron transfer to the Cr(VI) ion upon photoexcitation. Fig. 6 shows the optimized structures of a chromate(VI) ester adsorbed on the TiO_2 (101) and WO_3 (002) surfaces, and the charge densities of their HOMO and LUMO states. As shown in the figure, most of the contribution to the HOMO arises from the chromate(VI) ester for both cases. When photoexcited, the electron in the chromate(VI) ester would preferably inject into the oxide surface, as indicated by the high charge density of LUMO state in both the TiO_2 and WO_3 slabs. These results as well as the strong chromate(VI) ester adsorption on TiO_2 imply that it is thermodynamically possible that the interfacial charge injection interrupted the original inner sphere LMCT within the chromate(VI) ester (and subsequently the reduction of the Cr(VI) center). Despite the favorable interfacial electron injection from the chromate(VI) ester to WO_3, the weak adsorption may have limited such effect. This explains the weaker effects of the WO_3 compared to TiO_2 in retarding the Cr(VI) photoreduction.

Up to this point, we have considered the homogeneous photodecomposition and reduction of the chromate(VI) ester, as well as the negating effect of the interfacial electron injection. The latter clearly took place in the presence of 0.1 g L^{-1} of TiO_2 and WO_3 photocatalysts under full arc and visible light irradiations (Fig. 2). In principle, the surface photocatalytic reduction of Cr(VI) should take place, but kinetically this can only be measured when the yield of the photocatalytic reduction exceeds that of the homogeneous photodecomposition. To verify this, we conducted the photocatalytic reduction of Cr(VI) as a function of photocatalyst loadings. Indeed, as shown in Fig. 7, the rate of reduction of Cr(VI) under full arc irradiation increases with increasing TiO_2 concentration and even exceeds the homogeneous photodecomposition-reduction of Cr(VI) at TiO_2 loading of 0.5 g L^{-1} and above. Strictly speaking, increasing the TiO_2 photocatalyst loading also increases the surface sites for interfacial electron injection from the chromate(VI) ester to TiO_2 and this contributed to the initial decreasing rate up to 0.1 g L^{-1}, but at higher TiO_2 loading the rate of photocatalytic reduction of Cr(VI) becomes dominant (Fig. 7g, Scheme 1a and d).

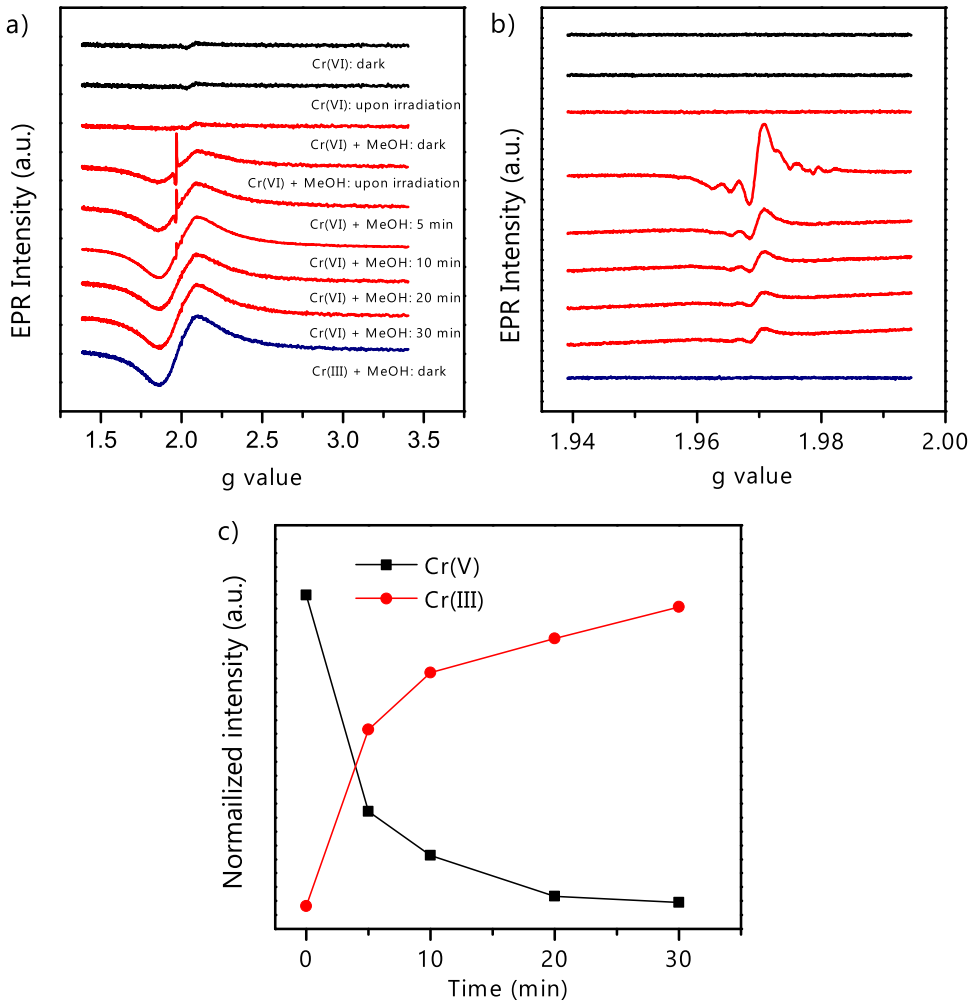

Fig. 9. (a) Wide scan and (b) enlarged EPR spectra of Cr(VI) + methanol in the dark, upon irradiation and at different irradiation time. Also shown are EPR spectra of the control Cr(VI) samples in the dark and upon irradiation, as well as Cr(III) + methanol reference sample. (c) Kinetic plot of the normalized intensities of EPR signals for Cr(III) and Cr(V) at different irradiation time. Initial Cr(VI) concentration = 1000 ppm, 12.5 M methanol, pH = 3.0, N_2 saturated, full arc Xe irradiation.

As expected, increasing Al_2O_3 loading had no effect on the rate of Cr(VI) reduction since no interfacial charge injection and transfer could take place (Scheme 1c). Similarly, increasing the WO_3 loading did not improve the Cr(VI) reduction since the chromate(VI) does not adsorb strongly on WO_3 for photocatalytic charge transfer to take place efficiently (Scheme 1b and e).

In accordance with our hypothesis, increasing (non-photoexcited) TiO_2 concentration under visible light irradiation essentially increases the surface area for the interfacial charge injection from chromate(VI) ester to TiO_2 conduction band. As a result, the Cr(VI) reduction rate was decreased ($k = 0.0035\ min^{-1}$ at $0.1\ g\ L^{-1}$, to $k = 0.0029\ min^{-1}$ at $0.5\ g\ L^{-1}$) (Fig. 8a and d and Scheme 1). Although the presence of WO_3 slightly suppressed the rate of Cr(VI) reduction, the difference when the photocatalyst loading was increased from 0.1 to $0.5\ g\ L^{-1}$ was rather insignificant, corroborating the weak electrostatic interactions between chromate(VI) ester and WO_3 surface (Fig. 8b,e,g and Scheme 1). As expected, the increase in Al_2O_3 concentration did not result in any significant effect on the rate of Cr(VI) reduction (Fig. 8c,f,g). Although a significant amount of initial adsorption of chromate ester could be measured on Al_2O_3, it did not affect the rate of Cr(VI) reduction (Fig. 8f and Scheme 1).

Lastly, to clarify reduction mechanism of chromate(VI) ester, we followed the evolution of chromate intermediate and product species using EPR spectroscopy. Since deionized water and methanol are diamagnetic, they have no features in EPR while the slight paramagnetism of the chromate(VI) ion is usually not detectable by EPR. On the other hand, the anticipated photoreaction products Cr(V) d^1, Cr(IV) d^2, and Cr(III) d^3 have one, two, and three unpaired electrons, respectively, and hence are expected to exhibit EPR spectra. As shown in Fig. 9, there is no signal for the mixed solution of Cr(VI) and methanol in the dark, and reconfirmed to be so even after 2 h (not shown). Upon irradiation, the spontaneous formation of paramagnetic species led to the appearance of two signals, one is ~400 gauss wide at g = 1.97 (Fig. 9a) and the other one is ~4 gauss wide at g = 2.2 (Fig. 9b). These results reaffirm that the chromate(VI) ester is photoactive, which is in line with our kinetics measurements and the earlier works by others [25,35,42,43]. By comparing the EPR spectrum of a reference mixed solution of Cr(III) and methanol, we confirm the broad signal at g = 1.97 as belonging to the Cr(III). The 4 gauss signal at g = 2.2 could be assigned to Cr(IV), Cr(V), or to organic radicals. The Cr(IV) specie has two unpaired *d* electrons and may form a triplet (S = 1) ground state. However, examination of the methyl chromate reaction did not reveal the signature transition of Cr(IV) triplet state at 77 K [42]. The 4 gauss signal is not split by hyperfine interaction, so it is not possible to positively determine whether the signal is due to an organic radical (which generally have narrow line widths). However, another possible assignment of the 4 gauss signal is to the formation of Cr(V) as an intermediate product of the photoreduction of Cr(VI). The evo-

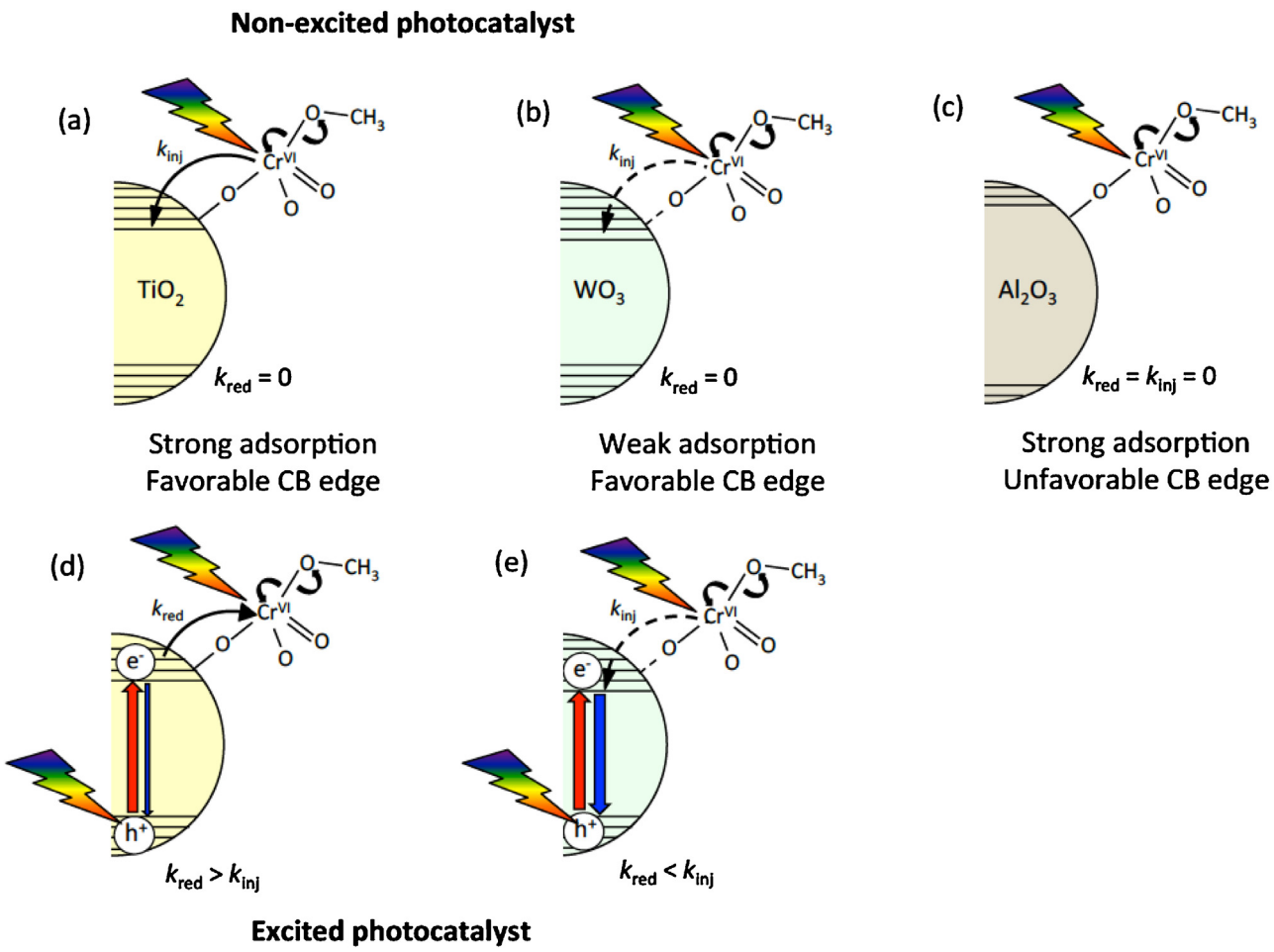

Scheme 1. The proposed interfacial charge transport process taking place between chromate(VI) ester and non-photoexcited (a) TiO_2, (b) WO_3 and (c) Al_2O_3, as well as the photoexcited (d) TiO_2 and (e) WO_3. For simplicity in (d) and (e), only the more dominant charge transport, *i.e.*, charge injection (k_{inj}) or surface reduction (k_{red}), is shown. The arrows with solid and broken lines denote fast and slow charge transport, respectively. Likewise, the weak bonding between chromate ester and WO_3 surface is represented by the broken line bond.

lution of proposed Cr(V) and Cr(III) are presented in Fig. 10c as a function of time of irradiation, which clearly shows that the intensity of Cr(V) declined with irradiation time, while the intensity of Cr(III) increased with irradiation time.

The evolution of Cr(V) and Cr(III) with the presence of 0.1 g L^{-1} TiO_2, WO_3 and Al_2O_3 are shown in Fig. 10. Compared to the solution with the absence of catalysts, the presence of TiO_2 or WO_3 retarded the formation of Cr(V), which is the first step to the reduction of chromate(VI) ester. This further led to the proportionally slower formation of Cr(III) end products.

4. Conclusions

We identified the spontaneous formation of photosensitive chromate(VI) ester upon the addition of methanol to aqueous Cr(VI). With absorbance up to 525 nm, its photoexcitation induces the LMCT that leads to the reduction of the stepwise Cr(VI) centre to Cr(III). The presence of TiO_2 at low concentrations (<0.5 g L^{-1}) interrupted the inner sphere electron transfer by inducing interfacial electron injection to the conduction band. As a result, the rate of Cr(VI) reduction was suppressed. This heterogeneous process requires the strong adsorption of the chromate(VI) ester on the TiO_2 surface, and in this case promoted by the strong electrostatic interactions. For this reason, the weak adsorption of chromate(VI) ester on the negatively charged WO_3 showed weaker effects compared to the TiO_2. Despite the interrupted electron transfer in the heteroge-

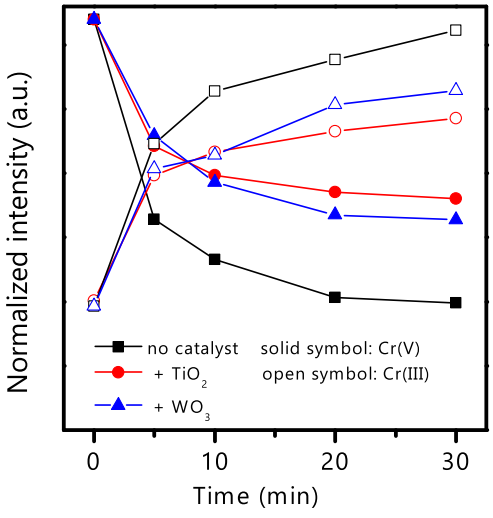

Fig. 10. Kinetic plot of the normalized EPR intensities for Cr(V) and Cr(III) without catalyst, and with 0.1 g L^{-1} TiO_2 or WO_3 as a function of irradiation time. All Cr(V) and Cr(III) intensities are normalized with respect to the initial and at the end of irradiation (30 min) of the homogeneous photoreduction, respectively. Initial Cr(VI) concentratio = 1000 ppm,12.5 M methanol, pH = 3.0, N_2 saturated, full arc Xe irradiation.

neous process, we confirmed that the reduction of Cr(VI) undergoes the same stepwise reduction from Cr(VI) to Cr(V) and finally to Cr(III). Although photoexcited TiO_2 is capable of direct photocatalytic reduction of Cr(VI), this effect only becomes dominant (*i.e.*, overcoming the negating interfacial electron injection) when the photocatalyst loading is higher than 0.5 g L^{-1}. With increased photocatalytic electron transfer sites, the rate of Cr(VI) reduction was 4 times higher than that of homogeneous reduction when TiO_2 loading is 1.0 g L^{-1}. Although we specifically showcase the chromate ester system in the current work, the non-independent effects of homogeneous photodecomposition and heterogeneous photocatalytic reduction may in fact be applicable to other systems involving a wider combination of metal ions and sacrificial organic electron donors [44]. In cases where photosensitive complexes are formed, the analyses of the photocatalytic reduction kinetics should be practised with care.

Acknowledgements

The authors thank Dr Jianping Xiao (Stanford University) for sharing the model for WO_3 crystal. The work was financially supported by the Research Grant Council of Hong Kong through the General Research Fund (Project 11337116).

Appendix A. Supplementary data

Supplementary data associated with this article can be found, in the online version, at http://dx.doi.org/10.1016/j.apcatb.2017.04.024.

References

[1] J.-M. Herrmann, Catal. Today 53 (1999) 115–129.
[2] X. Shi, Y. Mao, A.D. Knapton, M. Ding, Y. Rojanasakul, P.M. Gannett, N. Dalal, K. Liu, Carcinogenesis 15 (1994) 2475–2478.
[3] K. Salnikow, A. Zhitkovich, Chem. Res. Toxicol. 21 (2008) 28–44.
[4] I.A.R.C. Monogr, Eval. Carcinog. Risks Hum. 49 (1990) 1–648.
[5] S. Langård, Am. J. Ind. Med. 17 (1990) 189–215.
[6] H.J. Gibb, P.S. Lees, P.F. Pinsky, B.C. Rooney, Am. J. Ind. Med. 38 (2000) 115–126.
[7] A.S. Ellis, T.M. Johnson, T.D. Bullen, Science 295 (2002) 2060–2062.
[8] J.M. Davies, D.F. Easton, P.L. Bidstrup, Br. J. Ind. Med. 48 (1991) 299–313.
[9] J.J. Testa, M.A. Grela, M.I. Litter, Environ. Sci. Technol. 38 (2004) 1589–1594.
[10] N. Wang, L. Zhu, K. Deng, Y. She, Y. Yu, H. Tang, Appl. Catal. B: Environ. 95 (2010) 400–407.
[11] W.Y. Teoh, J.A. Scott, R. Amal, J. Phys. Chem. Lett 3 (2012) 629–639.
[12] X. Gong, G. Liu, Y. Li, D.Y.W. Yu, W.Y. Teoh, Chem. Mater. 28 (2016) 8082–8118.
[13] H. Yang, S.V. Kershaw, Y. Wang, X. Gong, S. Kalytchuk, A.L. Rogach, W.Y. Teoh, J. Phys. Chem. C. 117 (2013) 20406–20414.
[14] X. Gong, W.Y. Teoh, J. Catal. 332 (2015) 101–111.
[15] S. Chakrabarti, B. Chaudhuri, S. Bhattacharjee, A.K. Ray, B.K. Dutta, Chem. Eng. J. 153 (2009) 86–93.
[16] M.R. Prairie, L.R. Evans, B.M. Stange, S.L. Marlinez, Environ. Sci. Technol. 27 (1993) 1776–1782.
[17] G. Colón, M.C. Hidalgo, J.A. Navio, Langmuir 17 (2001) 7174–7177.
[18] L. Wang, N. Wang, L. Zhu, H. Yu, H. Tang, J. Hazard. Mater. 152 (2008) 93–99.
[19] E. Selli, A. De Giorgi, G. Bidoglio, Environ. Sci. Technol. 30 (1996) 598–604.
[20] C. Uyguner, Appl. Catal. B: Environ. 49 (2004) 267–275.
[21] G. Kim, W. Choi, Appl. Catal. B Environ. 100 (2010) 77–83.
[22] U.K. Kläning, J. Chem. Soc. Faraday Trans. 1: Phys. Chem. Condens. Phases 73 (1977) 434–455.
[23] U. Kläning, Acta Chem. Scand. 12 (1958) 807–813.
[24] U. Kläning, Acta Chem. Scand. 13 (1959) 2152–2154.
[25] F. Holloway, M. Cohen, F.H. Westheim, J. Am. Chem. Soc. 322 (1951) 1–4.
[26] W.Y. Teoh, F. Denny, R. Amal, D. Friedmann, L. Mädler, S.E. Pratsinis, Top. Catal. 44 (2007) 489–497.
[27] J. Lin, P. Hu, Y. Zhang, M. Fan, Z. He, C.K. Ngaw, J.S.C. Loo, D. Liao, T.T.Y. Tan, RSC Adv. 3 (2013) 9330–9336.
[28] J.P. Perdew, K. Burke, M. Ernzerhof, Phys. Rev. Lett. 77 (1996) 3865–3868.
[29] P. Giannozzi, S. Baroni, N. Bonini, M. Calandra, R. Car, C. Cavazzoni, D. Ceresoli, G.L. Chiarotti, M. Cococcioni, I. Dabo, A. Dal Corso, S. de Gironcoli, S. Fabris, G. Fratesi, R. Gebauer, U. Gerstmann, C. Gougoussis, A. Kokalj, M. Lazzeri, L. Martin-Samos, N. Marzari, F. Mauri, R. Mazzarello, S. Paolini, A. Pasquarello, L. Paulatto, C. Sbraccia, S. Scandolo, G. Sclauzero, A.P. Seitsonen, A. Smogunov, P. Umari, R.M. Wentzcovitch, J. Phys. Condens. Matter 21 (2009) 395502.
[30] D.T. Cromer, K. Herrington, J. Am. Chem. Soc. 77 (1955) 4708–4709.
[31] B.O. Loopstra, P. Boldrini, Acta Crystallogr. 21 (1966) 158–162.
[32] M.I. Litter, Appl. Catal. B: Environ. 23 (1999) 89–114.
[33] M.I. Litter, Treatment of Chromium, Mercury, Lead, Uranium, and Arsenic in Water by Heterogeneous Photocatalysis, Vol. 36, Elsevier, 2009.
[34] I.K. Levy, M. Mizrahi, G. Ruano, G. Zampieri, F.G. Requejo, M.I. Litter, Environ. Sci. Technol. 46 (2012) 2299–2308.
[35] S.H. Kaufman, J.M. Weber, J. Phys. Chem. A 117 (2013) 2144–2151.
[36] P. Mytych, P. Cie, Z. Stasicka, Int. J. Photoenergy 3 (2001) 181–186.
[37] P. Cieśla, P. Kocot, P. Mytych, Z. Stasicka, J. Mol. Catal. A Chem. 224 (2004) 17–33.
[38] A.D. Bokare, W. Choi, Environ. Sci. Technol. 45 (2011) 9332–9338.
[39] G. Kim, W. Choi, Appl. Catal. B: Environ. 100 (2010) 77–83.
[40] J. Kim, C.W. Lee, W. Choi, Environ. Sci. Technol. 44 (2010) 6849–6854.
[41] R. Abe, H. Takami, N. Murakami, B. Ohtani, J. Am. Chem. Soc. 130 (2008) 7780–7781.
[42] V.N. Lee, R. Farlee, Polym. Eng. Sci. 17 (1977) 359–365.
[43] U. Klaning, Acta Chem. Scand. 11 (1957) 1313–1316.
[44] W.Y. Teoh, R. Amal, L. Mädler, S.E. Pratsinis, Catal. Today 120 (2007) 203–213.